

INTEGRATED OPTICAL WAVEGUIDES

PACS numbers: 42.82.Bq; 42.82.Ds; 42.82.Et
DOI: 10.1070/QE2013v043n08ABEH015089

Analysis of light propagation for a crossing of thin silicon wires using vertical tunnelling coupling with a thick optical channel waveguide

A.V. Tsarev, E.A. Kolosovskii

Abstract. **Using silicon photonic wires in a silicon-on-insulator structure as an example, we examine the problem of crossings of thin, high-index-contrast channel waveguides. To ensure high optical wave transmission efficiency at as low a level of parasitic scattering as possible, we propose using a structure with vertical coupling between a thin tapered silicon waveguide and a thick polymer waveguide, separated by a thin buffer oxide layer. Numerical simulation is used to find conditions under which such a structure (3×90 μm in dimensions) ensures 98% and 99% transmission efficiency at ~1.55 μm in 35- and 26-nm spectral ranges, respectively, for direct propagation and 99.99% transmission in the transverse direction. The optical element in question is proposed for use in optical microchips with multiple channel waveguide crossings.**

Keywords: *integrated optics, optical waveguide, method of lines, finite-difference time-domain (FDTD) method, beam propagation method (BPM), nanophotonics.*

1. Introduction

Crossings of channel optical waveguides are used in many optical elements [1, 2]. In connection with this, various crossing designs have been the subject of extensive studies (see e.g. Refs [1–16]). The most challenging problem is to make crossings of high-index-contrast optical waveguides, which include silicon photonic wires in silicon-on-insulator structures, widely used in silicon photonics [3, 4]. Various approaches have been proposed for improving the quality of crossings (reducing the crossing loss and crosstalk). In particular, the scattering loss can be minimised by adjusting the crossing angle [5], utilising discrete subwavelength structures [6], varying the relative position of intersecting waveguides [7] and increasing the waveguide width in the intersection region [8–12]. Unfortunately, most of the known approaches have inherent limitations: a modest level of reflected signals and an undesirable level of radiation scattered to ambient media. This may degrade the performance of the device when there is a large number of waveguide crossings. A good solution to the problem of minimising crosstalk is to make waveguide crossings in different spatial layers. Energy transfer between two channel waveguides (main and auxiliary) located in different layers usually takes place in their tapered parts (adiabatic taper) owing to vertical coupling through a buffer layer. In the case of two polymer waveguides with a low refractive index contrast (2.5% and 0.3%), this approach ensures a transmission loss as low as −0.2 dB for 30 crossings [1]. Similar losses, but for one crossing, were demonstrated as well in high-index-contrast silicon photonic wires with tunnelling coupling between two oppositely directed tapered waveguides located under one another [13]. Practical implementation of this solution depends crucially on the ability to grow polysilicon and precisely fabricate two oppositely directed tapered waveguides in a strictly specified position relative to one another.

Recently, we have proposed an alternative, more technologically viable solution: to use an auxiliary thick two-mode channel waveguide with a low refractive index (based on the SU-8 polymer) [14–16]. Efficient energy transfer between the main waveguide (thin photonic wire with a high refractive index) and the upper, auxiliary waveguide (thick, low-index waveguide, e.g. from a polymer) occurs at narrowing edges of thin silicon waveguides. In particular, it has been shown that the efficiency of optical energy transfer from a thin silicon waveguide to a thick polymer waveguide and again to a thin silicon waveguide can be as high as 98% [14]. The purpose of this study is to examine this solution in greater detail and find conditions that maximise its efficiency.

2. Photonic wire crossing using vertical tunnelling coupling with a thick channel optical waveguide

The waveguide structure design that ensures an efficient crossing of small photonic wires is schematised in Fig. 1. The photonic wires have a silicon core surrounded by an oxide layer. The cross section (width) of the core decreases as the intersection region is approached. Since the refractive indices of silicon (3.478) and the polymer (1.56) differ drastically, far from the intersection region the modes of the thin and thick waveguides interact little because their optical fields overlap only slightly and the modes have a large phase mismatch. Along flow 1, the width of the silicon waveguide decreases, which is accompanied by wave field expulsion from the photonic wire. In this process, the effective refractive index of the fundamental mode gradually decreases and 'crosses' that of the polymer waveguide. The energy transfer between the lower and upper waveguides considerably increases because the phase matching condition can be fulfilled concurrently with an appreciable overlap of the interacting modes. As a

A.V. Tsarev, E.A. Kolosovskii A.V. Rzhanov Institute of Semiconductor Physics, Siberian Branch, Russian Academy of Sciences, prosp. Akad. Lavrent'eva 13, 630090 Novosibirsk, Russia; e-mail: tsarev@isp.nsc.ru, kolos@thermo.isp.nsc.ru

Received 15 January 2013; revision received 14 May 2013
Kvantovaya Elektronika **43** (8) 744–750 (2013)
Translated by O.M. Tsarev

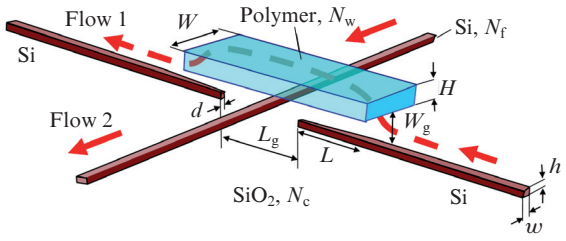

Figure 1. Schematic of an efficient crossing of two silicon wires. N_f, N_w and N_c are the refractive indices of the photonic wire core, polymer waveguide and oxide layer, respectively. L is the length of the silicon waveguide taper.

result, the optical wave can gradually tunnel through the buffer layer from the thin silicon waveguide to the thick polymer waveguide, thus overpassing the crossing with the silicon wire, and then return to the thin silicon waveguide.

The distance W_g between the broad, thick two-mode upper waveguide (based on the SU-8 polymer in our case) and the thin silicon wire should be large enough to allow the optical flow 2 (in the perpendicular direction) to freely pass through the intersection region. On the other hand, this distance should be small enough for the entire optical beam of flow 1, propagating along the wire, to tunnel to the thick polymer waveguide before the rupture and return to the wire after the crossing. To optimise silicon wire crossing parameters, one should find such structure parameters (d, h, w, H, W, L, L_g, N_w, N_f and N_c) that would ensure high transmission efficiency for flows 1 and 2 and low levels of backscatter and crosstalk between the two flows.

At the present stage, the problem of optical wave propagation through the inhomogeneous three-dimensional (3D) structure represented in Fig. 1 can be solved only numerically. We solved it for TE waves [14–16] by the finite-difference time-domain (FDTD) method [17]. Unfortunately, solving this problem in three dimensions is rather time-consuming (as a rule, several hours on a personal computer). Moreover, the optimisation problem is complicated by the large number of independent parameters, each of which can make a significant contribution to the efficiency of wave propagation through such a structure. Because of this, we used two-dimensional simulations wherever possible. In the final stage, 3D simulation was employed.

2.1. Two-dimensional simulation

To gain insight into the basic mechanisms that influence the energy exchange between different optical flows, it is convenient to utilise a 2D approximation of the problem and the effective refractive index method [18]. We are interested in two sections of the 3D structure, corresponding to flows 1 and 2, which were obtained with allowance for the specifics of the 2D approximation (Fig. 2).

The refractive indices $N_{h_1}(z)$ and $N_{h_2}(z)$ of the 2D silicon waveguide in the first structure (Fig. 2a) vary in the longitudinal direction (according to a parabolic law), which is optically equivalent to weakening of its guidance properties because of the reduction in the initial photonic wire width in the 3D configuration. Relations between parameters of the 2D and 3D waveguides can be found by comparing the dependences of their effective refractive indices N_{eff} on the width of the 3D

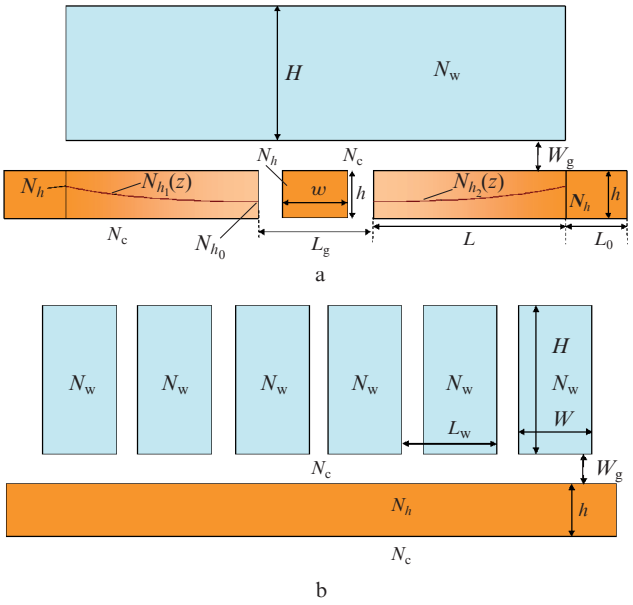

Figure 2. Two-dimensional representation of silicon wire crossings (a) for describing optical wave tunnelling from a thin waveguide to a thick one and back and (b) for describing optical wave propagation beneath the thick upper waveguide (crossing array).

waveguide and the minimum refractive index (N_{h_0}) of the core of the 2D waveguide (Fig. 3). For example, a silicon wire 330 nm in width and 0.22 μm in height can be represented in simulation as a 0.22-μm-high 2D waveguide with a refractive index $N_{h_0} = 2.19$. (The dashed line in Fig. 3 represents the correspondence algorithm for the requirement that the 2D and 3D waveguides have the same N_{eff}.)

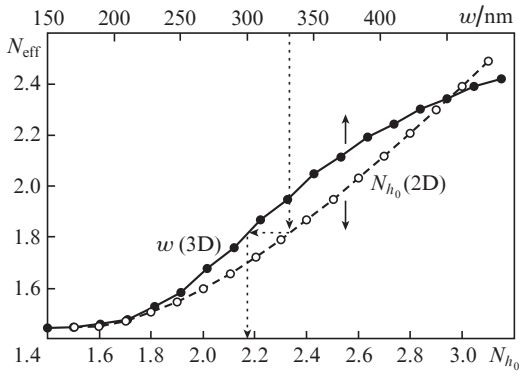

Figure 3. Effective refractive index N_{eff} of a silicon wire of height h = 0.22 μm as a function of its width w and refractive index N_{h_0} in 3D and 2D representations; W = 1.5 μm, H = 1.7 μm, N_f = 3.447, N_c = 1.4.

The second structure (Fig. 2b) is used to model multiple crossings for the optical flow 2 and analyse the tunnelling effect of polymer inserts on optical beam propagation in a 0.22-μm-high 2D silicon waveguide. Both structures require particular mathematical tools that would allow one to solve the 2D optical problem in the most reliable way. As the input parameters of the structures, we used parameters correspond-

ing to the optimal three-dimensional structure studied previously [14–16].

2.2. Application of the beam propagation method to analysis of energy exchange between the silicon and polymer waveguides

The propagation of the fundamental mode of the thin silicon waveguide through the structure shown in Fig. 2a was examined using the beam propagation method (BPM), which utilises a fourth-order Padé approximation [19]. Figure 4 illustrates the propagation of the fundamental mode of a channel silicon waveguide through this structure. It is seen that, as the intersection region (the middle of the structure) is approached, the optical wave gradually passes from the thin single-mode waveguide with a high refractive index to the auxiliary thick two-mode channel waveguide with a low refractive index. In this process, the field in the thick waveguide proves to be asymmetric and is largely the sum of the fields of its zeroth-order (TE_0) and first-order (TE_1) modes (Fig. 4b). Further propagating along the thick waveguide, the optical wave passes over the intersection region and tunnels back to the silicon wire in the form of its fundamental mode. In the central part of the structure, the field of the wave has a minimum ($T = 0$) on the axis of the thin waveguide, so there is another region with a high refractive index, corresponding to the second waveguide intersecting it. Under such conditions, there is negligible interaction between the waveguide being crossed and the incident wave, which ensures a low level of crosstalk.

Our analysis shows that the energy of the transmitted wave (flow 1) is determined not only by the amplitudes of the TE_0 and TE_1 modes excited in the upper waveguide through tunnelling coupling but also by the relationship between their phases (Fig. 5). The symmetry of the problem is such that, to optimise silicon wire crossing parameters, it is sufficient to examine the amplitudes of and the phase difference $\delta\varphi$ between the first two modes of the thick polymer channel waveguide in the centre of the structure (directly above the intersection region). The transmission of flow 1 has a maximum at $\delta\varphi \approx 0$, where both modes of the polymer waveguide subsequently transform, in the same phase, into the fundamental mode of the silicon wire. We have found the parameters of the structure that ensure an efficient silicon wire crossing for TE waves in the case of the upper layer consisting of the SU-8 polymer, with $N_w = 1.56$.

The adequacy of the model used is well illustrated by Fig. 6, which shows the efficiency of the transmission of the fundamental mode TE_0 through the intersection region of two silicon wires, evaluated by different methods. It can be seen that the 2D BPM results agree well with the FDTD direct numerical simulation data for the 2D waveguide. Note that, with increasing buffer layer thickness W_g, the maximum in efficiency takes place at a larger taper length L. In comparing the two- and three-dimensional models, it is reasonable to take into account the specifics of the two-dimensional approximation. Whereas relations between the parameters of the 2D and 3D waveguides can be established from the data in Fig. 3, comparison of their variations with buffer layer thickness

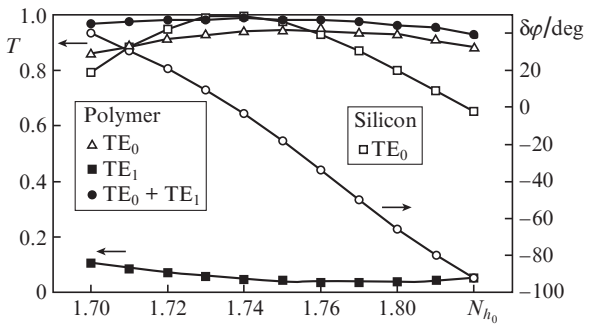

Figure 5. Fraction of the power carried by different modes of the two waveguides and phase difference $\delta\varphi$ between the first two modes of the thick polymer waveguide as functions of the refractive index N_{h_0} in the intersection region: calculation by the 2D BPM; $L_g = 3$ μm, $H = 1.7$ μm, $W_g = 180$ nm, $L = 45$ μm, $N_f = 3.447$, $N_w = 1.56$, $N_h = 2.95$, $N_c = 1.4$, $h = 220$ nm.

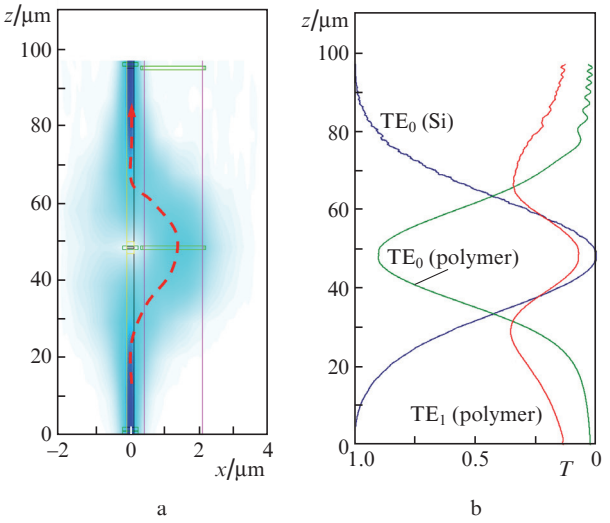

Figure 4. Tunnelling from a silicon wire to a polymer layer and back through the rupture region, as simulated by the 2D BPM: (a) transverse electromagnetic field distribution, (b) power distribution between modes along the axis of flow 1. $L_g = 3$ μm, $H = 1.7$ μm, $W_g = 80$ nm, $L = 45$ μm, $N_w = 1.56$, $N_h = 2.95$, $N_{h_0} = 1.76$, $N_c = 1.4$, $h = 220$ nm.

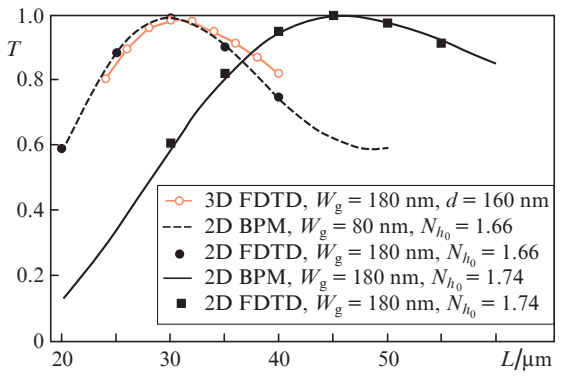

Figure 6. Efficiency of the transmission of the fundamental mode of a silicon waveguide through a structure composed of two coupled channel waveguides (Fig. 2a) vs. coupling length L, as evaluated by the BPM and FDTD method; $W = 1.5$ μm, $H = 1.7$ μm, $L_g = 3$ μm, $N_f = 3.447$, $N_w = 1.56$, $N_h = 2.95$, $N_c = 1.4$, $h = 220$ nm, $w = 450$ nm.

gives less clear results. It should be taken into account here that the transverse distributions of optical modes in the 2D and 3D waveguides differ drastically, so the maximum in energy transfer between different modes will also be observed at different W_g values. An important point for us is that, under optimal conditions, the efficiencies of wave transmission through the intersection region differ little, and the difference in transmission between the 2D and 3D waveguides reduces to a monotonic shift of optimal W_g values (Fig. 6).

Thus, the algorithm of the search for optimal parameters of three-dimensional silicon wire crossings can be reduced to the following procedure: The fast 2D BPM algorithm is used to find parameters of an optimal 2D structure, and it is convenient to end the search with the following sequence of steps: At given values of L and W_g, one seeks the optimal refractive index of the core of the 2D waveguide, N_{h_0} (Fig. 5). The results are then refined by varying W_g (Fig. 7). In doing so, different values of L will correspond to different combinations of optimal N_{h_0} and W_g. If the parameters thus found meet the criteria specified for the search (e.g. efficiency criteria), a three-dimensional analogue of the structure is sought. To this end, at a given value of L we analyse wave transmission through the intersection region of silicon wires by the more time consuming 3D FDTD method, first with variable d and then with variable W_g (at a predetermined optimal value of d).

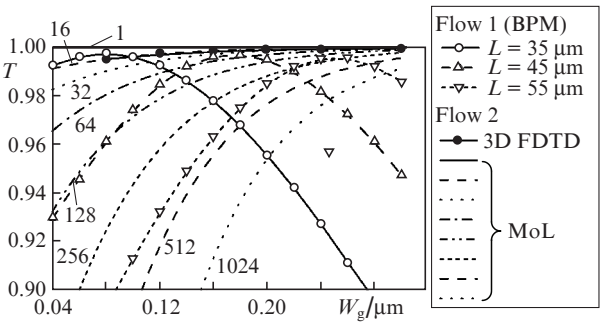

Figure 7. Efficiency of fundamental mode transmission through the structure schematised in Fig. 2b, as evaluated by the 3D FDTD method, 2D BPM and 2D MoL. The number of crossings for flow 2 is indicated at the curves. $L_g = 3$ μm, $W = 1.5$ μm, $H = 1.7$ μm, $L = 30$ μm, $N_f = 3.447$, $N_w = 1.56$, $N_h = 3.0$, $N_{h_0} = 1.56$, $N_c = 1.4$, $h = 220$ nm, $w = 450$ nm, $d = 160$ nm.

2.3. Application of the method of lines to analysis of a silicon waveguide crossing with a polymer waveguide array

As pointed out above, parasitic scattering of flow 2 should be made weak enough to be regarded as insignificant even in the case of a large number of similar crossings, necessary e.g. for producing optical multiplexers with coupled channel waveguides [20–22]. A method for quantitative analysis of the structure schematised in Fig. 2b should ensure high accuracy in assessing the scattered field at arbitrarily small disturbances of the fundamental mode of a thin silicon waveguide. This requirement can only be fully met by analytical methods.

The problem in hand corresponds to light propagation through a continuous silicon wire (Fig. 1, flow 2), with the polymer waveguide as perturbation. The BPM and FDTD method are in general poorly applicable in this case [23] because they are incapable of ensuring necessary accuracy. For this reason, the problem was solved using a version of the method of lines (MoL) – a specialised numerical–analytical approach employed by a number of researchers [23–27] to analyse high-index-contrast structures. The method was implemented as home-written software in which the analytical component was maximised to ensure high simulation accuracy.

The potentialities of the method of lines are well illustrated by Fig. 8, which shows the scattered field for optical wave transmission in the case of two polymer inserts located above the wire (see Fig. 2b). Since scattered fields are too weak to be seen, the field of the incident wave was subtracted from the resultant total field. As a result, in the structure of the wave field we can identify three downward optical flows, two back-reflected flows etc. It is seen that the MoL modelling results agree well with FDTD numerical simulation data, but in contrast to the FDTD method the MoL uses numerical–analytical algorithms, which allows one to obtained reliable results even for small perturbations, characteristic of the problem formulation for flow 2. Note that the results presented in Fig. 8 are at the accuracy limit of the FDTD method, so the tunnelling gap between the waveguides in the FDTD method was taken to be rather small ($W_g = 100$ nm) in order to increase the level of TE_0 mode scattering.

To further verify the MoL algorithm used, we compared it to the 3D FDTD direct simulation method, analysing the transmission of flow 2 for 16 crossings. The direct simulation results were in excellent quantitative agreement with the MoL results in Fig. 7. In those simulations, the spacing between the polymer inserts (L_w =2.2 μm) was adjusted so that the working wavelength (1.55 μm) strongly differed from the characteristic Bragg wavelengths corresponding to the periodic arrangement of the waveguides. Coherent effects can then be neglected, and the transmittance of a structure composed of many pairs of identical reflectors is the transmittance of one pair to the corresponding power: $T_n = T_2^{n/2}$,where T_2 and T_n are the transmittances of two and n reflectors, respectively (see Fig. 2b). The use of double rather than single reflectors allows reflection from the end faces of the polymer waveguides to be more adequately taken into account.

The data displayed in Fig. 7 demonstrate that, by optimising parameters of the structure, one can reach high transmission efficiency (above 98%) for both flows. Note that flow 2 can pass through an arbitrary number of similar silicon wire crossings (1 to 1024). Note also that the parameters L and W_g may depend on the number of crossings.

It is important to note that suboptimal conditions of efficient crossings can be reached at different combinations of parameters of the structure, which ensures sufficient freedom and the possibility of taking into account extra factors that influence the operation of a given optical element. In particular, transmission efficiency is a strong function of the thickness W_g of the buffer layer that divides the structure (see Fig. 7). If the size of the device (dependent on the coupling length L) should be minimised, the transmission reaches a maximum at a rather small layer thickness (W_g = 80 nm). As seen in Fig. 7, this buffer layer thickness is sufficient for reaching high (99.99%) transmission efficiency for flow 2. If the number of crossings is not too large (less than 16), the transmission efficiency for flow 1 is about 98%. At a larger number of crossings (above 32), it is necessary to reduce parasitic scat-

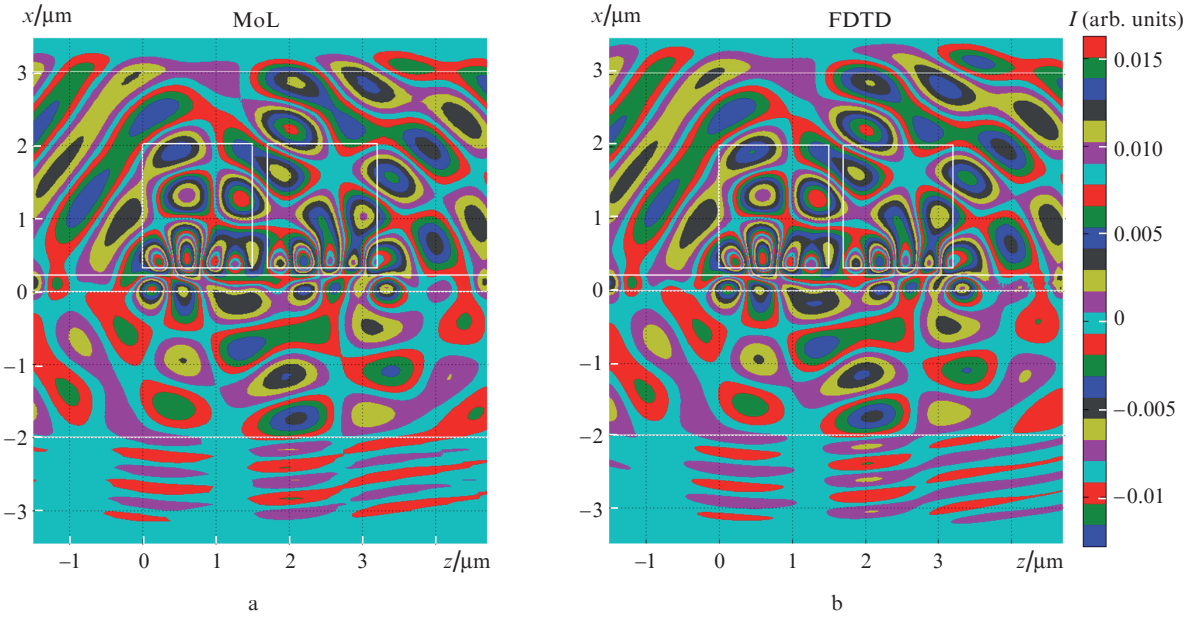

Figure 8. Scattered field distributions obtained by the (a) 2D MoL and (b) 2D FDTD method for fundamental mode propagation through a structure with two channel waveguide crossings; $L_g = 3$ μm, $W = 1.5$ μm, $H = 1.7$ μm, $W_g = 80$ nm, $L = 30$ μm, $N_f = 3.447$, $N_w = 1.56$, $N_h = 3.0$, $N_{h_0} = 1.56$, $N_c = 1.4$, $h = 220$ nm, $w = 450$ nm, $d = 160$ nm.

tering of flow 2 by increasing the buffer layer thickness. To maintain high overall transmission efficiency for flow 1, it is then reasonable to use longer structures ($L = 45$ or 55 μm), which satisfy the optimal transmission condition at a larger thickness ($W_g = 120$ or 230 nm, respectively). Analysis shows that, in this case, the transmission efficiency for flow 2 remains at an acceptable level (98%) at a considerably larger number of crossings (64 to 1024).

2.4. Three-dimensional simulation

A search for structure completes the 3D FDTD study of a three-dimensional element that ensures efficient silicon wire crossings. According to the procedure described above, the efficiency and minimum size (<100 μm) criteria chosen are satisfied by a structure with $L = 45$ μm, $W_g = 340$ nm and $d = 180$ nm. The spectral properties of the major optical flows through such a structure, normalised to the incident power, are presented in Fig. 9. The optical element in question has an extremely high efficiency, so to better illustrate our results we used the loss parameters Loss and Loss16, which specify the total fraction of energy lost when the fundamental mode of a silicon wire passes through the intersection region: Loss $= 1 - T_1$ and Loss16 $= 1 - T_{16}$, where T_1 is the relative output power for flow 1 and T_{16} is the relative output power for flow 2 having 16 crossings with flow 1. It is well seen that the optimal device ensures a transmission efficiency for flow 1 near 99% (Loss = 0.01) in a 26-nm spectral range and 98% in a broader (35 nm) telecommunications spectral range. In addition, it has very low levels of backscatter (Back) and crosstalk (Cross): less than –50 and –70 dB, respectively. Light scattering in flow 2 proved to be very weak – near the limit of the 3D FDTD method, so we analysed signal transmission simultaneously through 16 identical crossings spaced $L_w = 2.2$ μm apart. At this spacing, the Bragg reflections were located far from the working spectral range. It is seen that

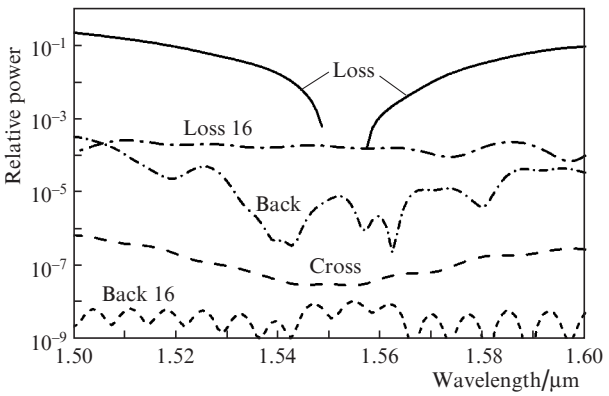

Figure 9. Relative TE_0 mode power as a function of wavelength for different flows; 3D FDTD calculations; Loss $= 1 - T_1$, Loss 16 $= 1 - T_{16}$; $L_g = 3$ μm, $W = 1.5$ μm, $H = 1.7$ μm, $W_g = 340$ nm, $L = 45$ μm, $N_f = 3.447$, $N_w = 1.56$, $N_h = 3.0$, $N_{h_0} = 1.56$, $N_c = 1.4$, $h = 220$ nm, $w = 450$ nm, $d = 180$ nm.

the loss (Loss 16) is extremely low, which can ensure up to 1700 analogous crossings at a total signal transmission of at least 98%. Thus, the proposed optical element can ensure transmission efficiency at a level of 98% for flow 1 and more than 1000 crossings for flow 2.

High transmission efficiency can be reached at an optimal combination of all parameters of the structure. Clearly, a deviation of any parameter from its optimal value reduces the overall efficiency. To evaluate the efficiency, it is convenient to utilise the fact that the efficiency is a quadratic function of structural parameters near the optimum. This allows us to estimate the accuracy in parameters of the structure that should be maintained for ensuring a given transmission efficiency. For definiteness, we performed 3D FDTD calculations of the range of basic parameters that ensure a 1% decrease in transmission efficiency for flow 1 at a fixed refrac-

tive index of the thick waveguide (N_w = 1.556 ± 0.004) and L = 32 μm. As expected, the most sensitive parameter is the minimum photonic wire width, d = 165 nm, which should be maintained with very high accuracy, about 2% (±4 nm). The parameters L and H should be maintained with an accuracy of about 6% (±2 and ±0.1 μm, respectively), and W, with an accuracy of 7% (±0.1 μm). The buffer layer thickness, W_g, responsible for the magnitude of tunnelling coupling, is the least sensitive (17%, or ±0.03 μm) to deviations in technology. It is seen that the parameters of the structure should meet rather stringent requirements for fabrication tolerances, which are, however, quite feasible for state-of-the-art nanophotonic technology with the use of deep-UV (193 nm) lithography. Note that, with allowance for the parabolic approximation used in the above analysis, increasing the fabrication tolerance by a factor of 2 reduces the transmission efficiency by 4%.

Note also that finding all parameters of a structure that ensures efficient crossings of optical silicon wires necessitates a trade-off between mutually exclusive requirements. Crucial for taking into account such requirements is the ability to rapidly and adequately calculate optical wave transmission in the two mutually perpendicular directions (flows 1 and 2). In view of this, the use of 2D simulation as a fast technique for solving a three-dimensional problem appears justified and probably the only possible in the case of multiple variations in parameters of the structure.

3. Conclusions

Crossings of thin single-mode silicon wires (with a high refractive index) using tunnelling coupling with a thick two-mode optical waveguide from a polymer (with a high refractive index) were analysed by parts, and different methodological approaches were used in each step.

The first part corresponds to direct fundamental mode transmission (flow 1), which involves transverse field energy transfer via vertical coupling (through an oxide layer) from the silicon waveguide taper to the upper thick channel polymer waveguide and back. This process was simulated using the BPM, and the results obtained agree well with direct simulation by the FDTD method.

The second part corresponds to a crossing (flow 2), where a silicon channel waveguide lies under a polymer insert, which is a two-mode waveguide in the first part of the problem. The key feature of the second part is very weak reflection from the polymer insert because of the small, tunnelling-induced disturbance of the optical flow. This determines another distinctive feature: the number of crossings can be very large (up to a thousand or even more). In this case, the BPM and FDTD method are poorly suited for analysis, so we used a semianalytical approach known as the method of lines (MoL), which proved very effective in the case of high-index-contrast structures.

Because of the large number of independent parameters (d, h, w, H, W, L, L_g, N_w, N_f and N_c), each of which can make a significant contribution to the efficiency of light transmission through the intersection zone, we tried to fully utilise the properties of 2D models. Three-dimensional simulation, which requires more resources in all respects, was used in the intermediate verification and final testing steps. A combined analysis of the problem by different methods (BPM, FDTD method, MoL and home-written software implementation of the MoL) allowed us to find combinations of parameters that ensured (in a 35-nm spectral range in the 1.55-μm telecom window) high crossing efficiency (at a level of 98% or even higher) for direct transmission (flow 1) and for the transverse direction (flow 2) with an arbitrary number (from 1 to 1024) of analogous crossings.

The optical elements described in this paper are quite technologically feasible. Crossings of high-index-contrast silicon wires with a polymer waveguide can be produced by CMOS-compatible nanophotonic technology [4, 28]. Such structures can find wide application in photonics and in designing novel optical microchips – whose operation is impossible without multiple crossings of optical microflows – and other devices, such as coupled-waveguide optical multiplexers [20–22].

Acknowledgements. We are grateful to RSoft Design Group Inc. for providing a user license for Rsoft Photonic CAD Suite 8.0 [29] for BPM and FDTD numerical simulation of integrated optical elements. This work was supported by the Russian Foundation for Basic Research (Grant No. 12-07-00018a).

References

1. Watanabe K., Hashizume Y., Nasu Y., Sakamaki Y., Kohtoku M., Itoh M., Inoue Y. *Electron. Lett*., **44**, 1356 (2008).
2. Shi W., Vafaei R., Torres M.Á.G., Jaeger N.A.F., Chrostowski L. *Opt. Lett*., **35**, 2901 (2010).
3. Reed G.T. *Silicon Photonics. The State of the Art* (Chichester: John Wiley & Sons, 2008).
4. Bogaerts W. et al. *J. Lightwave Technol*., **23**, 401 (2005).
5. Sanchis P., Galan J.V., Griol A., Marti J., Piqueras M.A., Perdigues J.M. *IEEE Photonics Technol. Lett*., **19**, 1583 (2007).
6. Bock P.J., Cheben P., Schmid J.H., Lapointe J., Delâge A., Xu D.-X., Janz S., Densmore A., Hall T.J. *Opt. Express*, **18**, 16146 (2010).
7. Tanaka D., Ikuma Y., Tsuda H. *IEICE Electron. Express*, **6**, 407 (2009).
8. Bogaerts W., Dumon P., Van Thourhout D., Baets R. *Opt. Lett*., **32**, 2801 (2007).
9. Chen H., Poon A. *IEEE Photonics Technol. Lett*., **18**, 2260 (2006).
10. Chen C.-H., Chiu C.-H. *IEEE J. Quantum Electron*., **46**, 1656 (2010).
11. Sanchis P., Villalba P., Cuesta F., Håkansson A., Griol A., Galán J.V., Brimont A., Martí J. *Opt. Lett*., **34**, 2760 (2009).
12. Fukazawa T., Hirano T., Ohno F., Baba T. *Jpn. J. Appl. Phys*., **43**, 646 (2004).
13. Sun R., Beals M., Pomerene A., Cheng J., Hong Ch.-Y., Kimerling L., Michel J. *Opt. Express*, **16**, 11682 (2008).
14. Tsarev A.V. *Opt. Express*, **19**, 13732 (2011).
15. Tsarev A.V. *Abs. 19th Intern. Workshop Optical Waveguide Theory and Numerical Modelling (OWTNM 2012)* (Barcelona, Spain, 2012) SaC2, p. 26.
16. Tsarev A. *Proc. 11th Intern. Conf. Actual Problems of Electronic Instrument Engineering (APEIE-2012*) (Novosibirsk, 2012) Vol. 1, p. 151.
17. Yee K.S. *IEEE Trans. Antennas Propag*., **AP-14**, 302 (1966).
18. Chiang K.S. *Appl. Opt*., **25**, 2169 (1986).
19. Lu Y.Y., Ho P.L. *Opt. Lett*., **27**, 683 (2002).
20. Tsarev A.V. *Abs. 19th Intern. Workshop on Optical Waveguide Theory and Numerical Modelling (OWTNM 2012)* (Barcelona, Spain, 2012) SaC2, p. 31.
21. Tsarev A. *Proc. 11th Intern. Conf. Actual Problems of Electronic Instrument Engineering (APEIE-2012)* (Novosibirsk, 2012) Vol. 1, p. 147.
22. Tsarev A. *Proc. SPIE Int. Soc. Opt. Eng.,* **8781**, 878106 (2013); http://dx.doi.org/10.1117/12.2017179.
23. Scarmozzino R., Gopinath A., Pregla R., Helfert S. *IEEE J. Sel. Top. Quantum Electron*., **6**, 150 (2000).

24. Pregla R., Pascher W. *The Method of Lines. Numerical Techniques for Microwave and Millimeter Wave Passive Structure* (New York: Wiley, 1989) p. 381.
25. Pregla R. *IEEE Microwave Guided Wave Lett*., **5**, 53 (1995).
26. Dreher A. *IEEE Africon*, **2**, 1049 (1999).
27. Hashish E.A., Saker H.A. *Proc. 21th Nat. Radio Sceince Conf.* (Cairo, 2004) sec.B14, p. 1.
28. Selvaraja S., Bogaerts W., Dumon P., Van Thourhout D., Baets R. *IEEE J. Sel. Top. Quantum Electron.*, **16**, 316 (2010).
29. www.rsoftdesign.com, Rsoft Photonic CAD Suite, ver. 8.0, single license (2007).